A mechanism-denial study on the Madden-Julian Oscillation with reduced interference from mean state changes

D. Ma,[1] and Z. Kuang[1,2]

Corresponding author: D. Ma, 20 Oxford St., Cambridge, MA 02138, USA. (dingma@fas.harvard.edu)

[1]Department of Earth and Planetary Sciences, Harvard University, Cambridge, Massachusetts, USA.

[2]School of Engineering and Applied Sciences, Harvard University, Cambridge, Massachusetts, USA.

Mechanism-denial experiments using Superparameterized Community Atmosphere Model are conducted to investigate the importance of extratropical and circumnavigating waves, wind-evaporation feedback and radiative-convective feedback to the Madden-Julian Oscillation (MJO). A common issue with mechanism-denial studies is the interference from mean state changes when processes are turned off in the model. Here, time-invariant forcing and nudging on effective timescales longer than the intraseasonal timescale are implemented to maintain the mean state. The MJO activity remains largely unchanged with suppressed extratropical and circumnavigating waves when the mean state is maintained to be close to that of the control run, suggesting that excitation of MJO by extratropical and circumnavigating waves is not necessary for the existence of MJO in this model. It is also shown that the wind-evaporation feedback slows down eastward propagation of the MJO, and the radiative-convective feedback amplifies the MJO.

1. Introduction

The Madden-Julian oscillation [MJO; Madden and Julian, 1971] is the dominant mode of intraseasonal variability in the tropics, and has been extensively studied in the past few decades [see, e.g., review by Zhang, 2005]. The characteristics of the MJO are well documented. The MJO features a spatial scale of zonal wavenumbers 1-3 and eastward propagation primarily in the Indian Ocean and western Pacific Ocean at around 5 m s^{-1}. Below we introduce the processes considered important to MJO initiation and maintenence in previous studies and examined here, including (i) surface heat fluxes and radiative fluxes, i.e., sources of the column-integrated moist static energy (hereafter column MSE) [e.g., Hu and Randall, 1994; Maloney et al., 2010; Andersen and Kuang, 2012], and (ii) influences of extratropical waves [e.g., Liebmann and Hartmann, 1984; Lau and Phillips, 1986] and circumnavigating waves [e.g., Knutson and Weickmann, 1987; Matthews, 2008].

The MJO has been hypothesized as a moisture mode in the sense that column moisture dominates the column MSE variations, and the growth and maintenance of the MJO is often interpreted in the context of processes recharging the column MSE while the MJO's propagation is sometimes viewed as the result of horizontal moisture advection which has been argued to lead column MSE [e.g., Fuchs and Raymond, 2002; Maloney et al., 2010; Sobel and Maloney, 2012; Sobel et al., 2014; Pritchard and Bretherton, 2014]. Wind-evaporation feedback and radiative-convective feedback are examples of such processes and are considered important to the MJO [e.g., Bony and Emanuel, 2005; Sobel et al., 2010]. With details different from the originally proposed linear theory [Emanuel, 1987; Neelin et al., 1987], surface heat flux anomalies, led by surface wind anomalies, are argued

to be positively correlated with the column MSE, and therefore strengthen the MJO [e.g., Maloney, 2009; Sobel et al., 2010; Kiranmayi and Maloney, 2011]. The radiative heating anomaly is found to be in phase with MJO precipitation and column MSE [Lin and Mapes, 2004; Ma and Kuang, 2011], and plays a significant role in maintaining the column MSE anomaly associated with the MJO [e.g., Andersen and Kuang, 2012; Sobel et al., 2014].

The recharge-discharge mechanisms for the MJO are internal to the tropics. However, coherence between the tropical convection and extratropical circulation on the intraseasonal timescale has been noticed since the 1980s [e.g., Weickmann, 1983; Lau and Phillips, 1986], and Hsu [1996] suggested that the intraseasonal oscillation is a global phenomenon. Despite controversy over the statistical significance of the dependence between the tropical and extratropical intraseasonal signals [Ghil and Mo, 1991], many studies tried to better understand the interactions between the oscillations in the tropics and those in the mid-latitudes. One direction of the interaction is through the propagation of Rossby waves generated by tropical heating, which leads to global responses [Jin and Hoskins, 1995; Matthews et al., 2004]. In the other direction, it has been observed that extratropical waves can propagate into the tropics in the regions with westerlies and lead to MJO initiation [e.g., Hsu et al., 1990]. Hoskins and Yang [2000] further showed that westerly winds are not necessary for extratropical influence on the tropical atmosphere because extratropical forcing can project onto the equatorial modes. More recent results from numerical integrations indicate that proper extratropical forcing leads to MJO initiation [Lin et al., 2007; Ray et al., 2009; Ray and Zhang, 2010]. In addition to extratropical waves, it has also been proposed that eastward circum-equatorial propagation of a Kelvin

wave caused by a preceding MJO event [e.g., Knutson and Weickmann, 1987; Matthews, 2008; Maloney, 2015].

Mechanism-denial experiments have been conducted in recent years to examine the importance of particular processes to the MJO [Kim et al., 2011; Ray and Li, 2013; Pritchard and Bretherton, 2014]. However, in these mechanism-denial studies, MJO response to the suppression of a particular process without being mediated by mean state changes is not distinguished from the response to the departure of mean state away from the control simulations, which leads to ambiguity in the interpretation. To examine the direct influences (i.e., without being mediated by mean state changes) of particular processes on the MJO, we have designed measures, largely inspired by Hall [2000], to minimize changes to the mean state when processes are disabled in the model. The methodology will be introduced in Section 2, including the model configuration, and experimental setup. In Section 3, we will first examine how the climatology and MJO activity respond in the experiments with suppressed extratropical waves, and use these experiments as an example to illustrate the importance of maintaining the mean state in mechanism-denial studies. The results from the other experiments are presented in the same section. A brief summary and further discussions follow in Section 4.

2. Methodology

2.1. Model

We used the Super-Parameterized Community Atmosphere Model [SPCAM; Khairoutdinov and Randall, 2001] Version 3.5, in which the conventional cloud parameterizations in the Community Atmosphere Model are replaced by a two-dimensional cloud system-

resolving model [Khairoutdinov and Randall, 2003]. SPCAM is chosen because it is known to produce robust MJO signals without tuning convection parameterization [e.g., Khairoutdinov et al., 2005; Andersen and Kuang, 2012; Benedict et al., 2014; Pritchard and Bretherton, 2014]. The simulations are conducted using semi-Lagrangian advection at T42 resolution (around 280 km) with 30 vertical levels on the Community Atmosphere Model level. On each grid point of the Community Atmosphere Model component, the embedded cloud-resolving array has 32 grid points that spans 128 km in the north-south direction. All the integrations are forced with perpetual February, the peak season of MJO activities [Zhang and Dong, 2004], sea surface temperature (Hadley Center Optimally Interpolated Sea Surface Temperature, averaged from 1980-2000). The simulations are integrated for 13 years and the first 3 years are discarded.

2.2. Experimental setup

Table 1 provides a brief description of the experiments. Inspired by Hall [2000], time-invariant forcing is applied to maintain the mean state. For each experiment, an ensemble of 28 simulations are restarted from different points of the CTL run, and integrated for 20 days. The first ensemble member restarts from the point where the CTL run has been integrated for six years, with each of the of following ensembles lagging the previous one by three months. Time-invariant forcing is computed using the tendency with which the ensemble mean drifts away from the climatology of the CTL run, and then applied to the next set of ensemble simulations. After four such iterations, the forcing can mostly compensate for the effects of the processes turned off. We also nudged the prognostic variables in the tropics back to the control run climatology on effective timescales longer

than the intraseasonal timescale to make sure the mean state is well maintained in a long-term integration (see Supporting Information for details).

To constrain the impact of the nudging described in the Supporting Information, NDG is integrated with the prognostic variables nudged back to the mean state of CTL. In CHN and CHNn, the intraseasonal disturbance can grow and propagate within a wide channel in the tropics, as the prognostic variables are relaxed towards the control run climatology north of 30°N and south of 40°S . The relaxation rate starts from zero at 30°N and 40°S, and increases linearly poleward till 42°N and 52°S, respectively, so that the waves emanating from the tropics are not reflected back. Poleward of 42°N and 52°S, the relaxation time is fixed at 9 hours. These latitudes are chosen so that the damping reaches sufficiently low latitudes to adequately suppress the extratropical waves, but does not extend too far into the tropics and suppress the patterns (e.g., Rossy gyres) associated with the MJO. The procedure to maintain the climatology is applied to all the experiments discussed in this paper, except CHNn (and CTL), so the climatology of the CHNn run can be substantially different from that of the CTL run. Comparison of CHNn and CHN runs highlights the interference due to changes to the climatology. To test the sensitivity to the latitudes beyond which the extratropical waves are suppressed, the equatorward boundaries of the relaxation zones are shifted from 30°N and 40°S to 10°N and 30°S in CHN2, leaving a narrower channel compared to CHN. In the experiment BOX, we further relax the prognostic variables toward the control run climatology all over the globe except within the box over the tropical Indian and Pacific Oceans (40°S-30°N, 0°E-270°E), so that both extratropical waves and circumnavigating waves are suppressed. In addition,

radiative-convective (wind-evaporation) feedback is turned off by prescribing the radiative heating (surface fluxes) using the control run climatology in the RAD (FLUX) experiment. Again, the climatologies of all experiments except CHNn (and CTL) are maintained to be that of the CTL run.

3. Results

The CTL run simulates the climatology reasonably well compared to observations. The precipitation maxima are located in the western Indian Ocean, the Maritime Continent and the western Pacific Ocean between 20°S and the Equator, as it is forced by perpetual February sea surface temperature (Figure 1A). The time-space power spectrum of the Outgoing Longwave Radiation (OLR) is calculated with successive 90-day segments of data overlapping by 60 days in the fashion of Wheeler and Kiladis [1999]. The power spectrum of precipitation is calculated in the same way and shown in the Supporting Information, confirming that OLR is a good proxy for deep convection. The peak at small wavenumbers and low frequencies in the spectrum shows a robust MJO signal in the CTL run (Figure 2A). The MJO bandpass filtered (30-90 days, wavenumbers 1-3) variance of OLR (Figure 1A) and precipitation (Figure S2A) indicate that the peak of MJO activity spans the Indian Ocean and the western Pacific Ocean between 20°S-8°S, a few degrees poleward compared to observations during boreal winter [e.g., Zhang, 2005]. When the prognostic variables are nudged on effective timescales longer than the intraseasonal timescale, the mean precipitation remains similar to that of the CTL run. While the tropical transients of the lowest resolved frequency (1/90 cpd) are damped (Figure 2B), the spatial distribution of MJO activity is also largely unchanged (Figure 1B). Despite

that the power spectrum is dominated by a flat peak at wavenumbers 1-4, the frequency-wavenumber diagram confirms that the simulation produces a strong MJO signal when the nudging is implemented (Figure 2B). Regressed MJO precipitation and 850 hPa wind anomalies also show realistic life cycle of MJO (see Supporting Information for details).

We now turn to the responses of the mean states and MJO activity in the experiments with suppressed extratropical waves, and these experiments will serve as an example to highlight the importance of maintaining the mean states. In CTL, there are large values of eddy momentum flux convergence in the midlatitudes (Figure 3A), as Rossby waves originating from these latitudes propagate into the tropics and the polar regions. When the extratropical waves are suppressed, the eddy momentum flux convergence disappears in the Northern Hemisphere, while there is still weak eddy momentum flux convergence on the equator flank of the damping zone (the equatorward boundary is marked by the dashed line) in the Southern Hemisphere (Figure 3B). When the extratropical waves are damped starting from lower latitudes, there is a single peak of eddy momentum flux convergence in the upper atmosphere lying over the tropics (Figure 3C), and it confirms that the extratropical waves are adequately suppressed. In fact, the responses of the MJO are similar in both the wide channel (CHN) and the narrow channel (CHN2) experiments, so only results from CHN will be shown hereafter.

The CTL run produces a strong cross-equatorial winter cell (Figure 4A), and the magnitude of the Hadley Cells matches reanalysis data well [Schneider, 2006]. When the extratropical waves are suppressed, the Hadley Cells and Ferrel Cells weaken (Figure 4B) if the mean state is not maintained (the CHNn run). In contrast, there is hardly any

changes in the circulation over the tropics in CHN, and it suggests that the method implemented in the present study is indeed able to minimize the departure of the mean states away from the CTL run. The response of the climatological precipitation shares a similar picture. As the Hadley Cells weaken in CHNn, the precipitation shifts poleward. The precipitation decreases over the Inter Tropical Convergence Zone, especially over the Equatorial Indian Ocean, and increases over the South Pacific Convergence Zone (Figure 1C), while the precipitation in CHN remains similar to that of the CTL run. The averaged precipitation over the domain with high MJO activity (between 25°S-10°N and 30°E-120°W) is 6.0 $mm\ day^{-1}$ in CTL, which is maintained to be the same in CHN, and reduced by 15% in CHNn. The pattern correlation between the precipitation in CTL and CHNn is 0.916, compared to 0.995 between that in CTL and CHN. Although the MJO signal seems to change little in the wavenumber-frequency spectrum (Figure 2C), the OLR variance of MJO decreases significantly in the Indian Ocean in CHNn (Figure 1C). As long as the climatology does not change, the spatial distribution of the MJO activity remains broadly unchanged even when the extratropical waves are suppressed (Figure 1D). The power spectrum also confirms that there is a strong signal of MJO without extratropical influence (Figure 2D). The regressed MJO precipitation and low-level winds anomales are concentrated over western Pacific in CHNn, while the MJO life cycle in CHN compares well with that in NDG and CTL (Figure S4-5).

The mean states are well maintained in BOX, FLX and RAD, in which the averaged precipitation is 6.0, 6.1 and 5.9 $mm\ day^{-1}$, and the pattern correlation of the precipitation with that in CTL is 0.994, 0.993 and 0.994, respectively. The influences of the circum-

navigating waves, wind-evaporation feedback and radiative-convective feedback can thus be assessed with reduced interference from mean state changes. Suppressing extratropical waves and circumnavigating waves barely changes the spatial distribution of MJO activity (Figure 1E). As the disturbances are suppressed over the Atlantic sector, the OLR power spectrum is dominated by a peak at zonal wavenumbers 2-3 (Figure 2E). The essential processes of the MJO are internal to the Equatorial Indian Ocean and the Pacific Ocean in the experiment BOX, as MJO initiation and maintenance are limited within these regions in the BOX experiment. The activity of the eastward propagating intraseasonal disturbances with planetary scales weakens significantly in FLX and RAD (Figure 1FG), which implies that the wind-evaporation feedback and radiative-convective feedback are important to the MJO. In FLX, the spectral peak shifts to higher frequency compared to the other experiments (Figure 2F), which indicates that the wind-evaporation feedback slows down MJO propagation in SPCAM. The MJO signal largely disappears in the power spectrum of the OLR when the radiative feedback is disabled (Figure 2G), in agreement with Kim et al. [2011]. On the other hand, the Kelvin wave becomes stronger without interactive radiative heating in RAD, consistent with the results from Andersen and Kuang [2012].

4. Summary and discussions

MJO mechanism-denial experiments have been conducted in a few recent studies [e.g., Ray and Li, 2013], in which, particular processes are disabled in numerical models, and the importance of these processes to the MJO and evaluated based on how MJO responds in the simulations. The response of MJO in these studies can be decomposed into two parts:

(1) response to mean state changes and (2) direct response to the suppression of certain process without being mediated by mean state changes. Using SPCAM, the present study seeks to examine the direct influences of the extratropical and circumnavigating waves, wind-evaporation feedback and radiative-convective feedback on the MJO with reduced interference from mean state changes. Using time-invariant forcing, combined with nudging the prognostic variables back to the control run climatology on effective timescales longer than the intraseasonal timescale, we were able to minimize the changes to the climatology from CTL when processes are eliminated or suppressed in the model. Without maintaining the climatology, the strength of the general circulation and tropical precipitation is reduced in response to suppressed extratropical waves as seen in Ray and Li [2013]. In particular, precipitation and MJO activity decrease significantly over the Indian Ocean. It is worth noting here the response of the mean state and MJO activity to the suppression of extratropical waves in CHNn is somewhat different from that in the simulations in Ray and Li [2013], which may be attributed to, besides model difference, the fact that the simulations are forced with perpetual February sea surface temperature in the present study, while the simulations in Ray and Li [2013] are integrated with annual cycle. The MJO activity remains generally the same as in the CTL run when the mean state change is minimized, leading to the conclusion that excitation of MJO by extratropical eddies are not essential for the existence of the MJO. This contrast highlights the importance of reducing the interference from mean state changes in mechanism-denial experiments. Results also suggest that the processes important to the MJO are internal to the tropical Indian and Pacific Oceans in SPCAM, because the simulation produces strong

MJO signals when the transients can only grow and propagate within these regions. The wind-evaporation feedback is found to slow down MJO propagation in the model. When the radiative-convective feedback is turned off, the MJO signal weakens significantly.

As the results show that excitation of MJO by extratropical and circumnavigating waves are not necessary for MJO's existence, it leads to the open question that how the present results can be reconciled with previous studies, in which the influences of extratropical and circumnavigating waves are argued to be important to MJO initiation. It is possible that the extratropical waves and circumnavigating waves determine the timing for some MJO initiation events, but the collective effects of the waves over a long period have little influence on MJO climatology. Besides, the circumnavigating waves might play a more significant role in MJO amplitude in idealized models such as that used by Maloney [2015]. The wind-evaporation feedback is shown to slow down the MJO, which is consistent with reanalysis data and numerical studies [Kiranmayi and Maloney, 2011; Maloney, 2009]. In an idealized simulation of the MJO [Andersen and Kuang, 2012], the surface flux is found to project positively onto the tendency of the column MSE, and the difference is attributed to the mean surface easterly winds in the idealized simulation, compared to the weak to westerly winds in the observations and realistic simulations. One caveat with the present study is the simulations are forced with fixed sea surface temperature, while it has been argued that including air-sea coupling in SPCAM can produce more realistic phasing between surface flux and precipitation and improve the simulated MJO [Benedict et al., 2011]. The radiative-convective feedback amplifies the MJO not only because, in the active phase of the MJO, the anomalous column-integrated radiative heating serves as

a direct source of column MSE, but also due to the bottom-heavy profile of the radiative heating anomaly [Ma and Kuang, 2011], which generates a bottom-heavy vertical velocity profile and can further import MSE into the column. In contrast, such bottom-heavy radiative heating anomaly in the convectively active phase weakens the Kelvin wave, as the stratiform instability for convectively coupled waves counts on top-heavy convective heating [Mapes, 2000; Kuang, 2008]. Also, a radiative-convective instability involving the interaction among radiative heating, water vapor, clouds and large-scale circulation has been proposed recently [Emanuel et al., 2014; Wing and Emanuel, 2014], and observational and numerical studies are needed to relate this instability to realistic MJO initiations.

Acknowledgments. This research was supported by NASA grant NNX13AN47 and DOE grant DE-SC0008464. D.M. thanks Jeffrey Shaman and Nathan Arnold for helping with model configuration. The authors thank two anonymous reviewers for the constructive reviews and the Harvard FAS Science Division Research Computing Group for computing support. The model data and modified routines of the model will be available upon request.

References

Andersen, J. A. and Z. Kuang, 2012: Moist static energy budget of MJO-like disturbances in the atmosphere of a zonally symmetric aquaplanet. *Journal of Climate*, **25 (8)**, 2782–2804, doi:10.1175/JCLI-D-11-00168.1.

Benedict, J. and D. Randall, 2011: Impacts of idealized air-sea coupling on Madden-Julian Oscillation structure in the superparameterized CAM, **68**, 1990–2008.

Benedict, J., E. Maloney, A. Sobel and M. Dargan, 2014: Gross moist stability and MJO simulation skill in three full-physics GCMs, **71**, 1990–2008.

Bony, S. and K. A. Emanuel, 2005: On the role of moist processes in tropical intraseasonal variability : cloud-radiation and moisture-convection feedbacks. *Journal of the Atmospheric Sciences*, **62**, 3327–3349.

Emanuel, K. A., 1987: An air-sea interaction model of intraseasonal oscillations in the tropics. *Journal of the Atmospheric Sciences*, **44**, 2324–2340.

Emanuel, K. A., A. Wing, and E. M. Vincent, 2014: Radiative-convective instability. *Journal of Advances in Modeling Earth Systems*, **5 (November)**, 1–13, doi: 10.1002/2013MS000270.

Fuchs, Z. and D. J. Raymond, 2002: Large-scale modes of a non-rotating atmosphere with water vapor and cloud-radiation feedbacks. *Journal of the Atmospheric Sciences*, **59**, 1669–1679.

Ghil, M. and K. Mo, 1991: Intraseasonal oscillations in the global atmosphere. Part i: Northern Hemisphere and tropics. *Journal of the Atmospheric Sciences*, **48 (5)**, 752–779.

Hall, N. M. J., 2000: A simple GCM based on dry dynamics and constant forcing. *Journal of the Atmospheric Sciences*, **57 (10)**, 1557–1572.

Hoskins, B. J. and G.-Y. Yang, 2000: The equatorial response to higher-latitude forcing. *Journal of the Atmospheric Sciences*, **57 (9)**, 1197–1213.

Hsu, H.-H., 1996: Global view of the intraseasonal oscillation during northern winter. *Journal of Climate*, **9**, 2386–2406.

Hsu, H.-H., B. J. Hoskins, and F.-F. Jin, 1990: the 1985/86 intraseasonal oscillation and the role of the extratropics. *Journal of the Atmospheric Sciences*, **47**, 823–839.

Hu, Q. and D. A. Randall, 1994: Low-frequency oscillations in radiative-convective systems. *Journal of the Atmospheric Sciences*, 1089–1099.

Jin, F.-F. and B. J. Hoskins, 1995: The direct response to tropical heating in a baroclinic atmosphere. *Journal of the Atmospheric Sciences*, **52 (3)**, 307–319.

Khairoutdinov, M. and D. A. Randall, 2001: A cloud resolving model as a cloud parameterization in the NCAR Community Climate System Model : preliminary results. *Geophysical Research Letters*, **28 (18)**, 3617–3620.

Khairoutdinov, M. and D. A. Randall, 2003: Cloud resolving modeling of the ARM summer 1997 IOP: model formulation, results, uncertainties, and sensitivities. *Journal of the Atmospheric Sciences*, **60 (4)**, 607–625.

Khairoutdinov, M., D. A. Randall, and C. DeMott, 2005: Simulations of the atmospheric general circulation using a cloud-resolving model as a superparameterization of physical processes. *Journal of the Atmospheric Sciences*, **62**, 2136–2154.

Kim, D., A. H. Sobel, and I.-S. Kang, 2011: A mechanism denial study on the Madden-Julian Oscillation. *Journal of Advances in Modeling Earth Systems*, **3**, M12007, doi: 10.1029/2011MS000081.

Kiranmayi, L. and E. D. Maloney, 2011: Intraseasonal moist static energy budget in reanalysis data. *Journal of Geophysical Research: Atmospheres*, **116 (21)**, D21117, doi:10.1029/2011JD016031.

Kuang, Z., 2008: A moisture-stratiform instability for convectively coupled waves. *Journal of the Atmospheric Sciences*, **65**, 834–854.

Knutson, T. R. and K. M. Weickmann, 1987: 30-60 day atmospheric oscillations: compostie life cycles of convection and circulation anomalies. *Monthly Weather Review*, **115**, 1407–1436.

Lau, K. M. and T. J. Phillips, 1986: Coherent fluxtuactions of extratropical geopotential height and tropical convection in intraseasonal time scales. *Journal of the Atmospheric Sciences*, **43**, 1164–1181.

Liebmann, B. and D. L. Hartmann, 1984: An observational study of tropical-midlatitude interaction on intraseasonal time scales during winter. *Journal of the Atmospheric Sciences*, **41**, 3333–3350.

Lin, H., G. Brunet, and J. Derome, 2007: Intraseasonal variability in a dry atmospheric model. *Journal of the atmospheric sciences*, **64 (7)**, 2422–2441.

Lin, J.-L. and B. E. Mapes, 2004: Radiation budget of the tropical intraseasonal oscillation. *Journal of the Atmospheric Sciences*, **61**, 2050–2062.

Ma, D. and Z. Kuang, 2011: Modulation of radiative heating by the Madden-Julian Oscillation and convectively coupled Kelvin waves as observed by CloudSat. *Geophysical Research Letters*, **38 (21)**, L21813, doi:10.1029/2011GL049734.

Madden, R. A. and P. R. Julian, 1971: Dectection of a 40-50 day oscillation in the zonal wind in tropical pacific. *Journal of the Atmospheric Sciences*, **28**, 7102–708.

Maloney, E. D., 2009: The moist static energy budget of a composite tropical intraseasonal oscillation in a climate model. *Journal of Climate*, **22 (3)**, 711–729, doi:

10.1175/2008JCLI2542.1.

Maloney, E. D., A. H. Sobel, and W. M. Hannah, 2010: Intraseasonal variability in an aquaplanet general circulation model. *Journal of Advances in Modeling Earth Systems*, **2**, 5, doi:10.3894/JAMES.2010.2.5.

Maloney, E. D., B. Wolding, 2015: Initiation of an intraseasonal oscillation in an aquaplanet general circulation model. *Journal of Advances in Modeling Earth Systems*, accepted, doi:10.1002/2015MS000495.

Mapes, B., 2000: Convective inhibition, subgrid-scale triggering energy, and stratiform instability in a toy tropical wave model. *Journal of the Atmospheric Sciences*, **57**, 1515–1535.

Matthews, A. J., 2008: Primary and successive envents in the Madden-Julian Oscillation. *Quarterly Journal of the Royal Meteorological Society*, **134**, 439–453, doi:10.1002/qj.

Matthews, A. J., B. J. Hoskins, and M. Masutani, 2004: The global response to tropical heating in the Madden-Julian oscillation during the northern winter. *Quarterly Journal of the Royal Meteorological Society*, **130**, 1991–2011 doi:10.1256/qj.02.123.

Neelin, J. D., I. M. Held, and K. H. Cook, 1987: Evaporation-wind feedback and low-frequency variability in the tropical atmosphere. *Journal of the Atmospheric Sciences*, **44**, 2341–2348.

Pritchard, M. S. and C. S. Bretherton, 2014: Causal evidence that rotational moisture advection is critical to the superparameterized Madden-Julian Oscillation. *Journal of the Atmospheric Sciences*, **71 (2)**, 800–815, doi:10.1175/JAS-D-13-0119.1.

Ray, P. and T. Li, 2013: Relative roles of circumnavigating waves and extratropics on the MJO and its relationship with the mean state. *Journal of the Atmospheric Sciences*, **70 (3)**, 876–893.

Ray, P. and C.. Zhang, 2010: A case study of the mechanics of extratropical influence on the initiation of the MaddenJulian Oscillation. *Journal of the Atmospheric Sciences*, **67 (2)**, 515–528, doi:10.1175/2009JAS3059.1.

Ray, P., C. Zhang, J. Dudhia, and S. S. Chen, 2009: A numerical case study on the initiation of the MaddenJulian Oscillation. *Journal of the Atmospheric Sciences*, **66 (2)**, 310–331, doi:10.1175/2008JAS2701.1.

Schneider, T., 2006: The general circulation of the atmosphere. *Annual Review of Earth and Planetary Sciences*, **34 (1)**, 655–688, doi:10.1146/annurev.earth.34.031405.125144.

Sobel, A. H., E. D. Maloney, G. Bellon, and D. M. Frierson, 2010: Surface fluxes and tropical intraseasonal variability: a reassessment. *Journal of Advances in Modeling Earth Systems*, **2**, 2, doi:10.3894/JAMES.2010.2.2.

Sobel, A. H., S. Wang, and D. Kim, 2014: Moist static energy budget of the MJO during DYNAMO. *Journal of the Atmospheric Sciences*, **71**, 4276–4291, doi:10.1175/JAS-D-14-0052.1.

Sobel, A. H. and E. D. Maloney, 2012: An idealized semi-empirical framework for modeling the Madden-Julian Oscillation. *Journal of the Atmospheric Sciences*, **69 (5)**, 1691–1705, doi:10.1175/JAS-D-11-0118.1.

Weickmann, K. M., 1983: Intraseasonal circulation and outgoing longwave radiation modes during Northern Hemisphere winter. *Monthly Weather Review*, **5**, 1838–1858.

Table 1. Brief description of the experiments. See text for details.

	process disabled	time-invariant forcing	nudging
CTL	n/a	×	×
NDG	n/a	×	√
CHNn	extratropical waves outside of 30°N and 40°S	×	×
CHN	extratropical waves outside of 30°N and 40°S	√	√
CHN2	extratropical waves outside of 10°N and 30°S	√	√
BOX	extratropical wave outside of 30°N and 40°S and circumnavigating waves	√	√
FLX	wind-evaporation feedback	√	√
RAD	radiative-convective feedback	√	√

Wheeler, M. C. and G. N. Kiladis, 1999: Convectively coupled equatorial waves : analysis of clouds and temperature in the wavenumber-frequency domain. *Journal of the Atmospheric Sciences*, **56**, 374–399.

Wing, A. and K. A. Emanuel, 2014: Physical mechanisms controlling self-aggregation of convection in idealized numerical modeling simulations. *Journal of Advances in Modeling Earth Systems*, **5**, 1–14, doi:10.1002/2013MS000269.

Zhang, C., 2005: Madden-Julian Oscillation. *Reviews of Geophysics*, **43**, 2004RG000158, doi:10.1029/2004RG000158.1.INTRODUCTION.

Zhang, C. and M. Dong, 2004: Seasonality in the Madden-Julian Oscillation. *Journal of Climate*, **17**, 3169–3180.

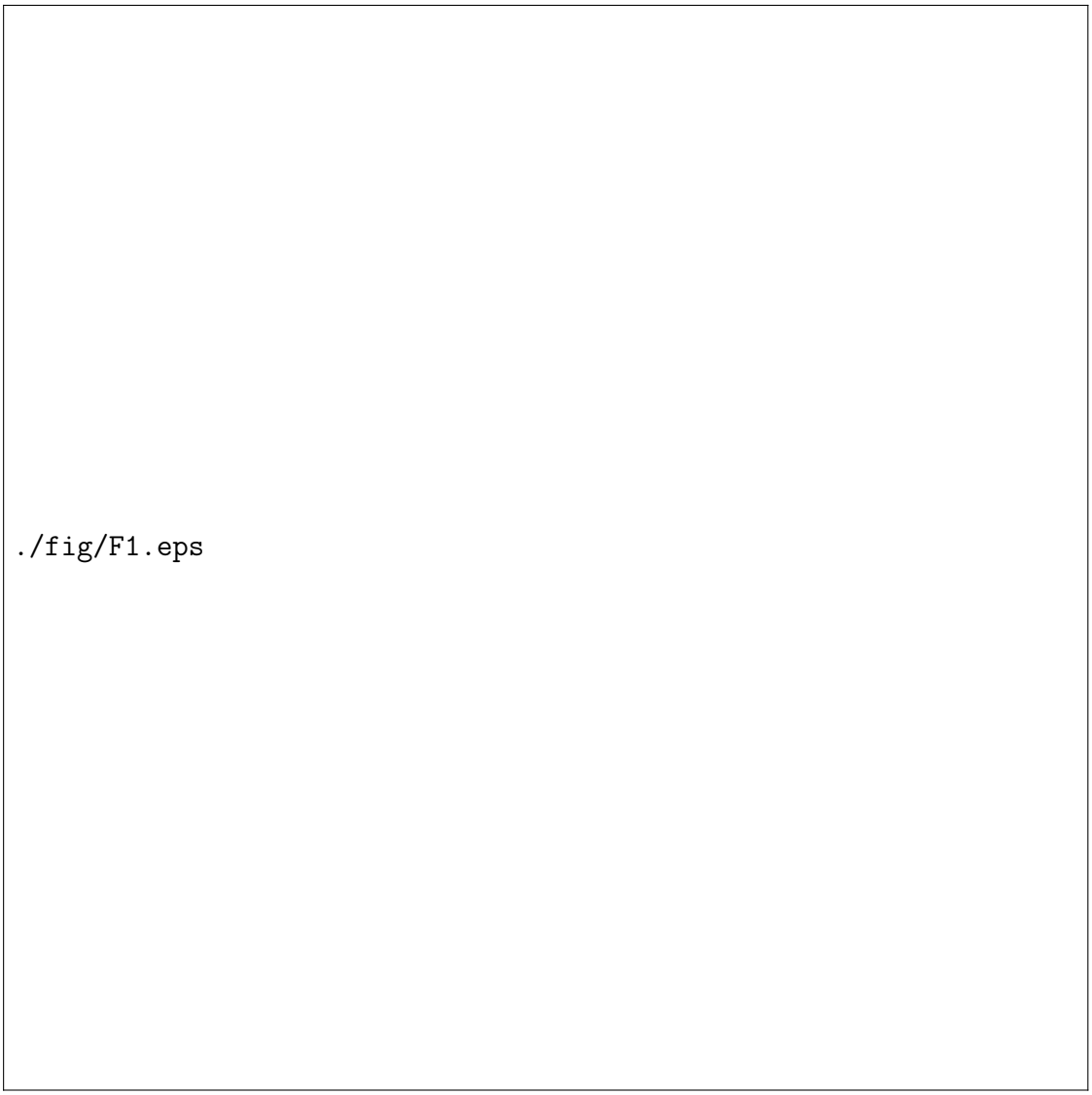

Figure 1. Mean precipitation (shaded) and OLR variance of the MJO (black contours) from the (A) CTL, (B) NDG, (C) CHNn, (D) CHN, (E) BOX, (F) FLX and (G) RAD. The silver contours denote the coast lines.

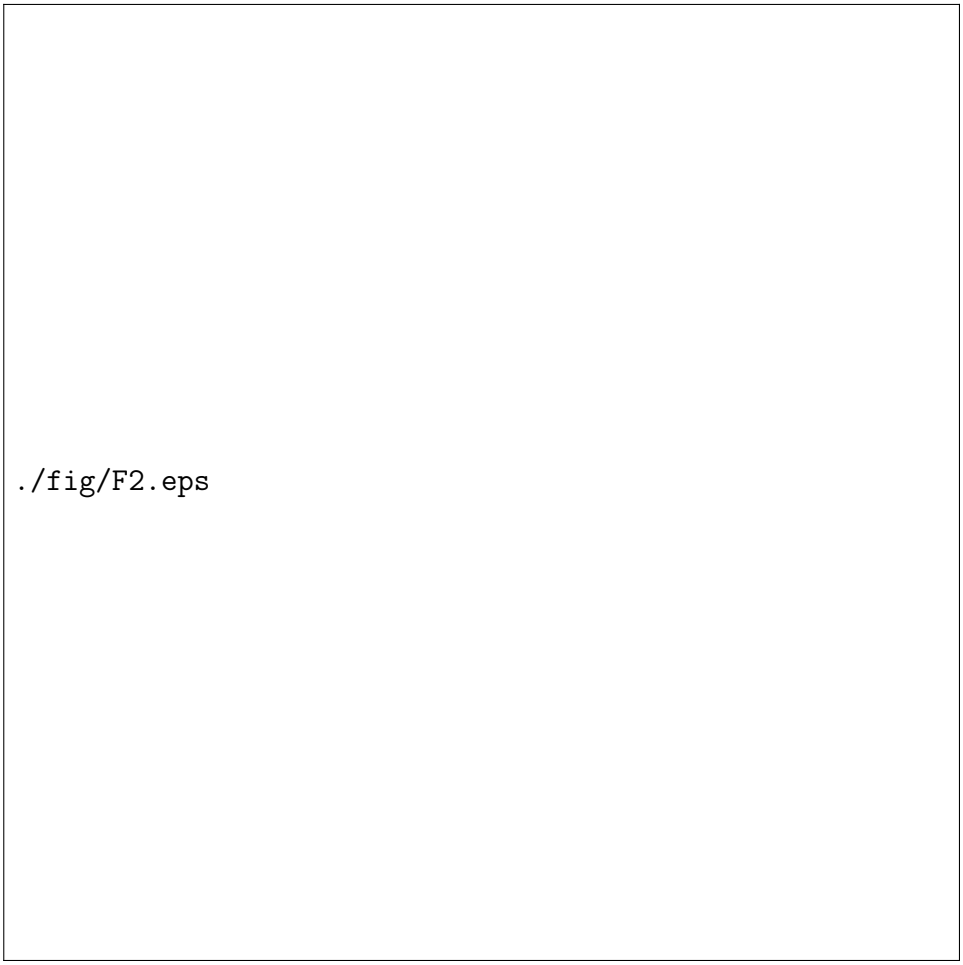

Figure 2. Time-space power spectra of the OLR averaged between 20°S-0° of (A) CTL, (B) NDG, (C) CHNn, (D) CHN, (E) BOX, (F) FLX and (G) RAD.

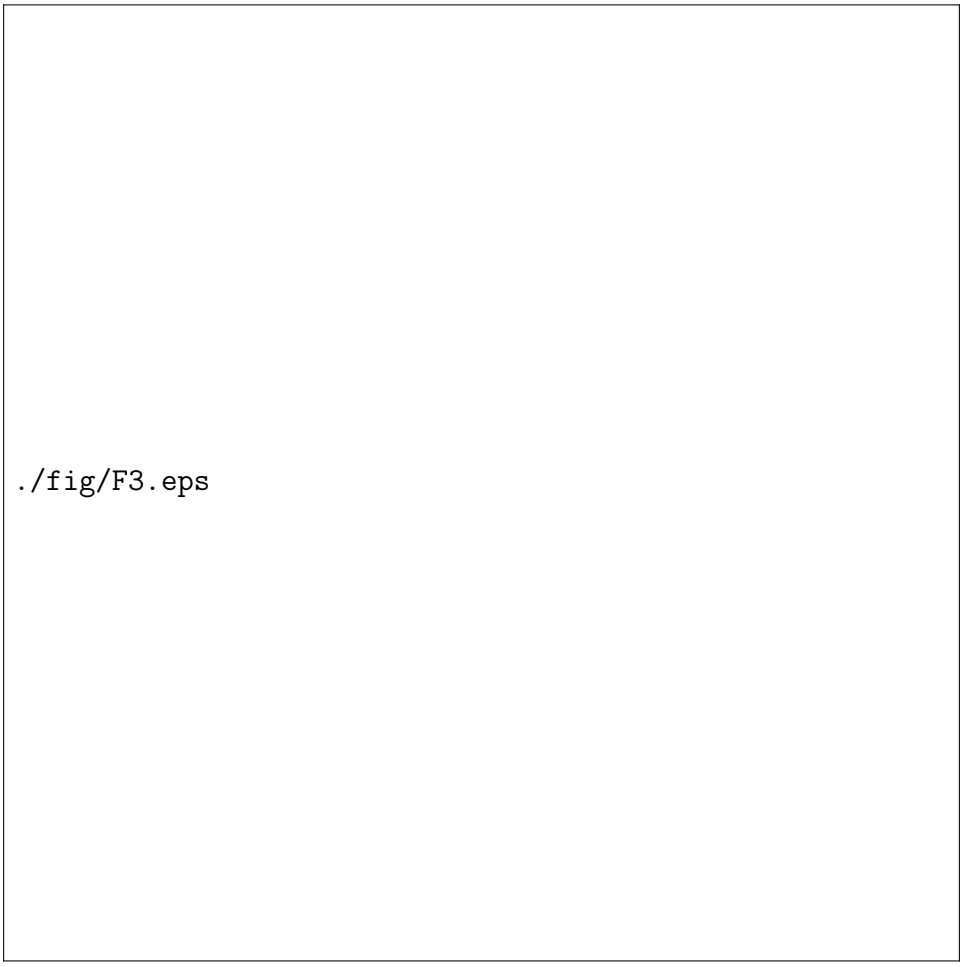

Figure 3. Temporal and zonal mean eddy forcing in (A) CTL, (B) CHN and (C) CHN2. In (B) and (C), the dashed lines denote the latitudes starting from which the extratropical eddies are damped. The relaxation rate increases linearly poleward till the solid lines, and remains constant poleward from the solid lines.

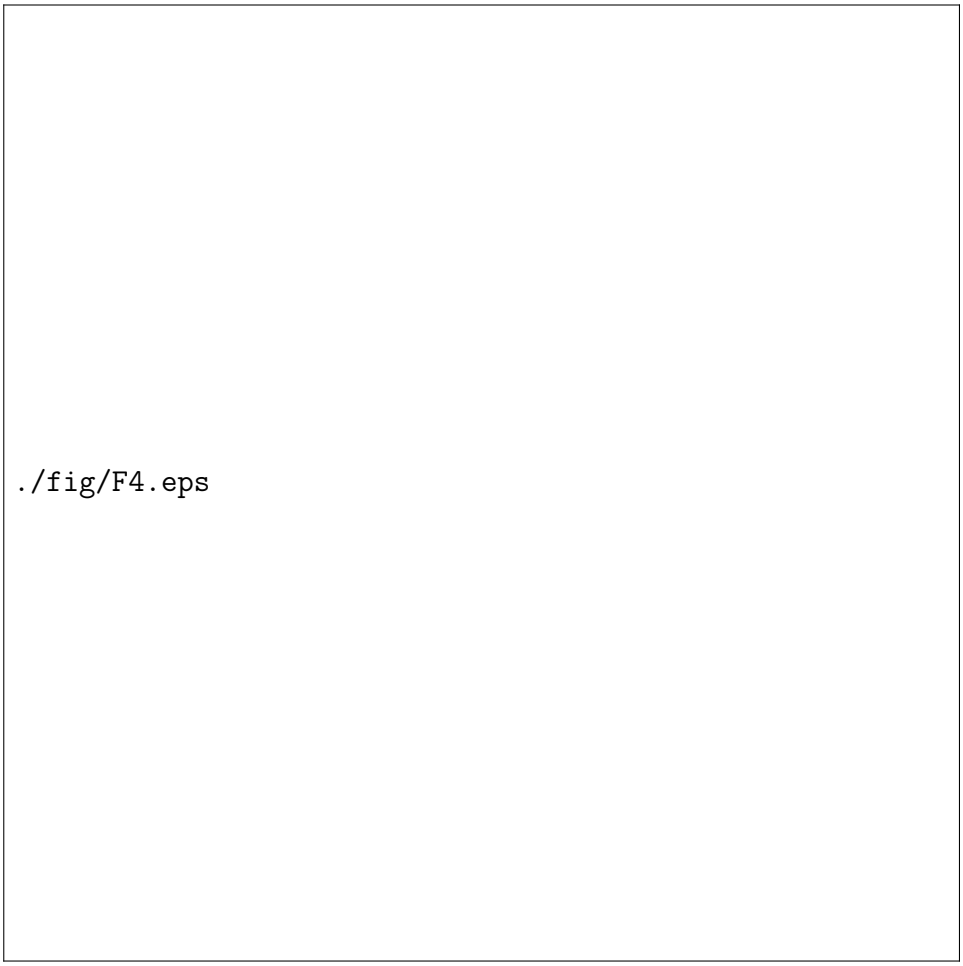

Figure 4. Temporal and zonal mean circulation in (A) CTL, and anomalous circulation in (B) CHNn and (C) CHN. Negative streamfunction values (dashed contours) correspond to clockwise circulation, and positive streamfunction values (solid contours) correspond to counter-clockwise circulation.

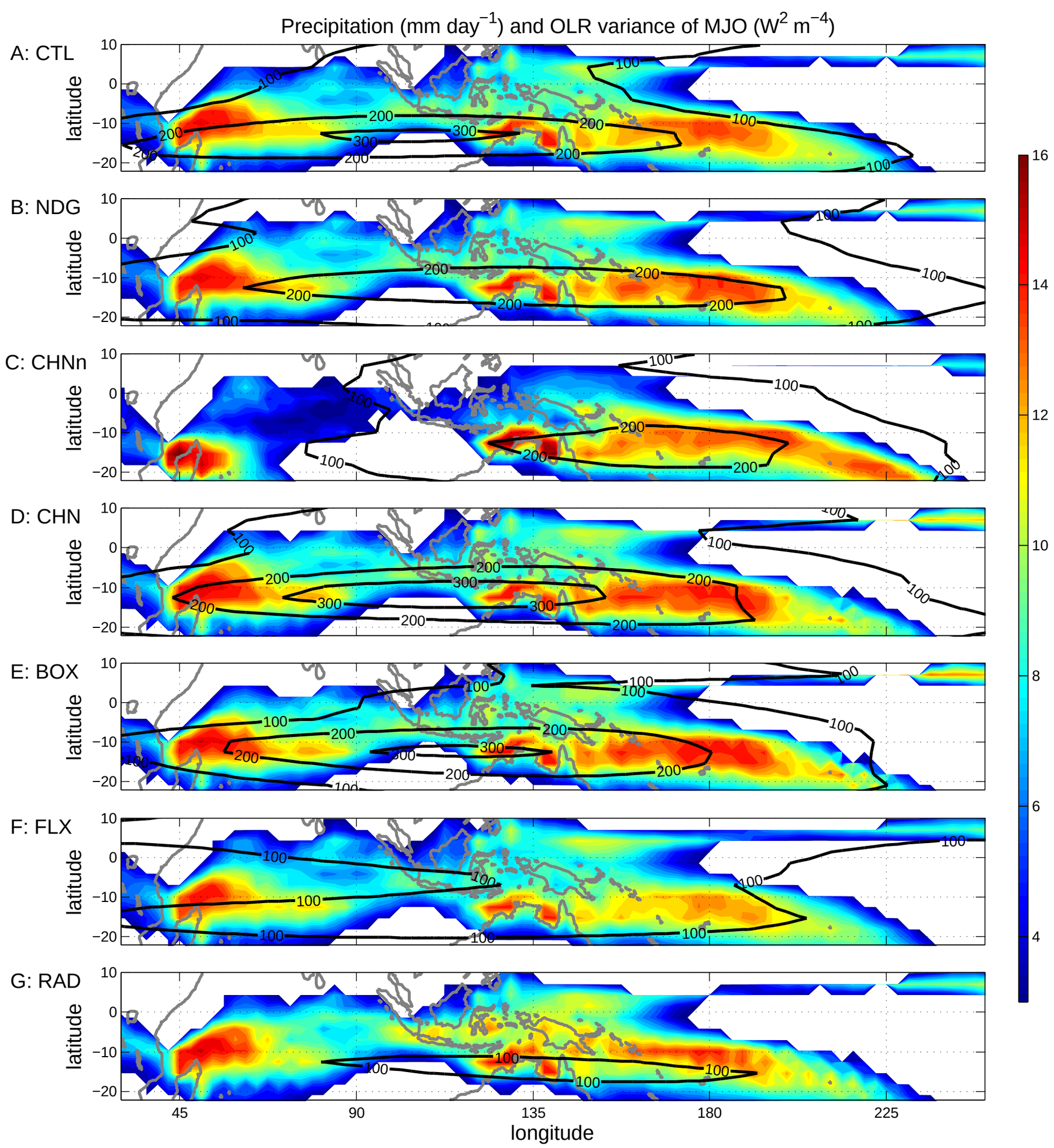
Precipitation (mm day^{-1}) and OLR variance of MJO (W^2 m^{-4})
A: CTL
B: NDG
C: CHNn
D: CHN
E: BOX
F: FLX
G: RAD
latitude
longitude
10
0
−10
−20
45
90
135
180
225
100
200
300
16
14
12
10
8
6
4

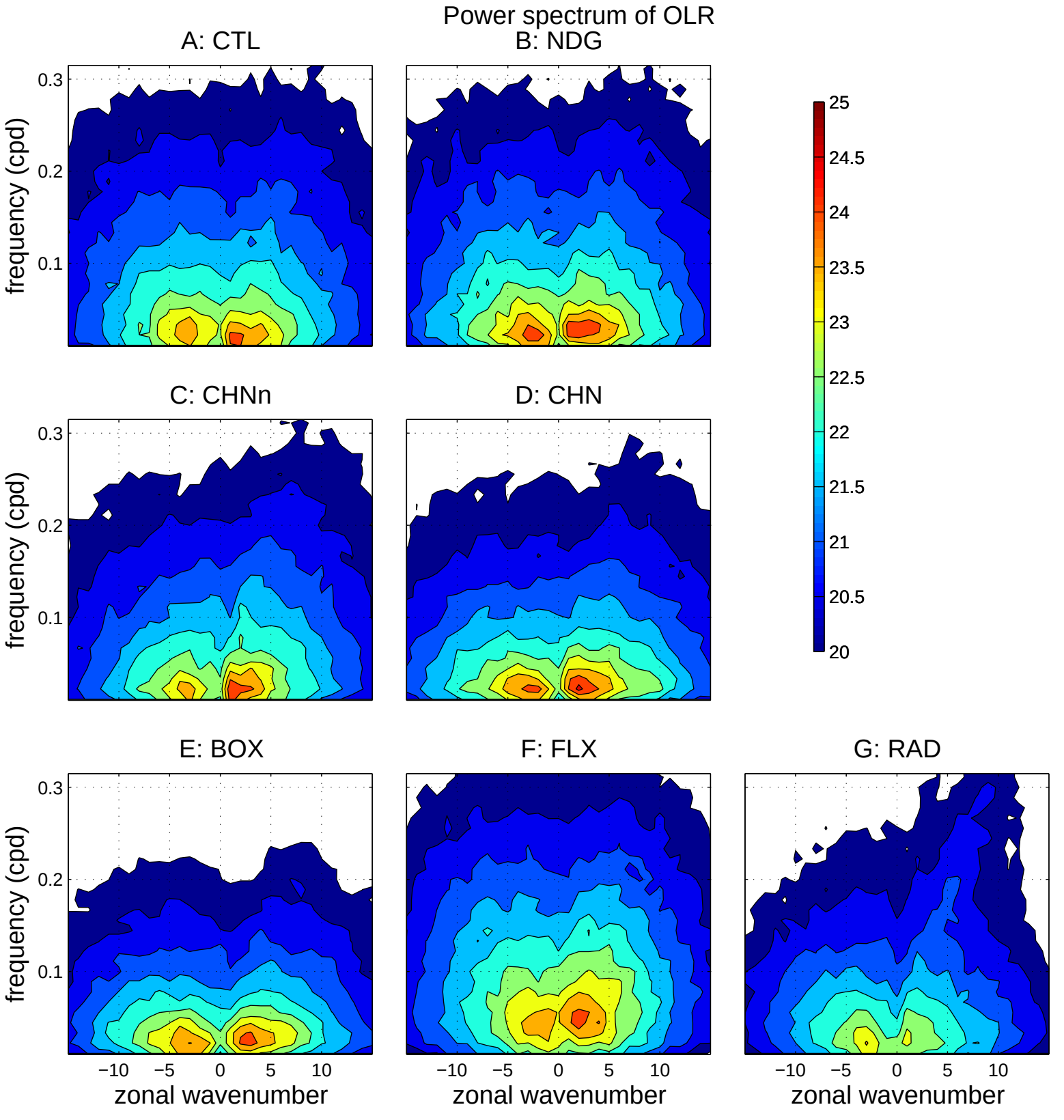
Power spectrum of OLR
A: CTL
B: NDG
C: CHNn
D: CHN
E: BOX
F: FLX
G: RAD
frequency (cpd)
0.3
0.2
0.1
25
24.5
24
23.5
23
22.5
22
21.5
21
20.5
20
−10
−5
0
5
10
zonal wavenumber

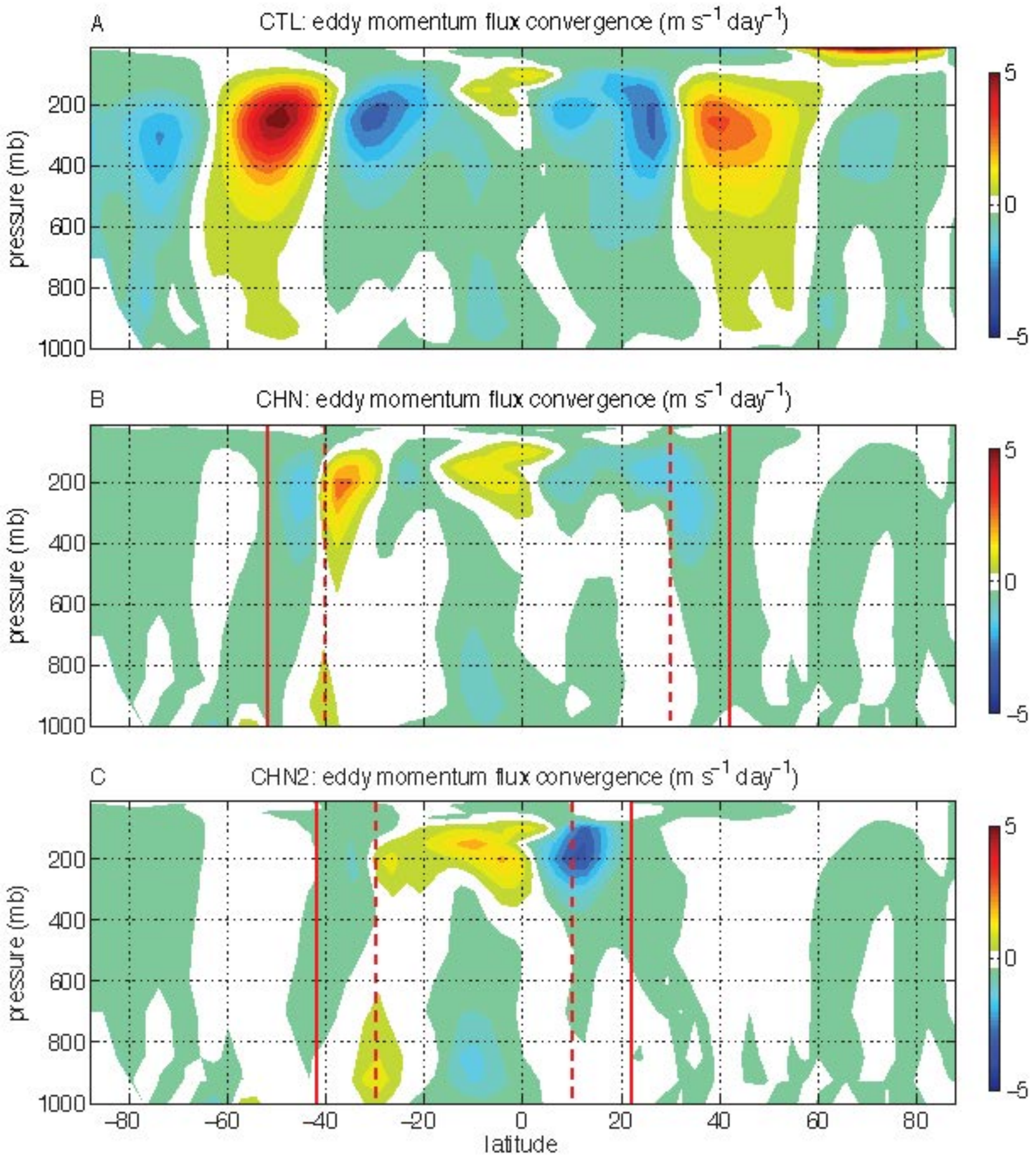
A
CTL: eddy momentum flux convergence (m s^{-1} day^{-1})
B
CHN: eddy momentum flux convergence (m s^{-1} day^{-1})
C
CHN2: eddy momentum flux convergence (m s^{-1} day^{-1})
pressure (mb)
200
400
600
800
1000
5
0
−5
−80
−60
−40
−20
0
20
40
60
80
latitude

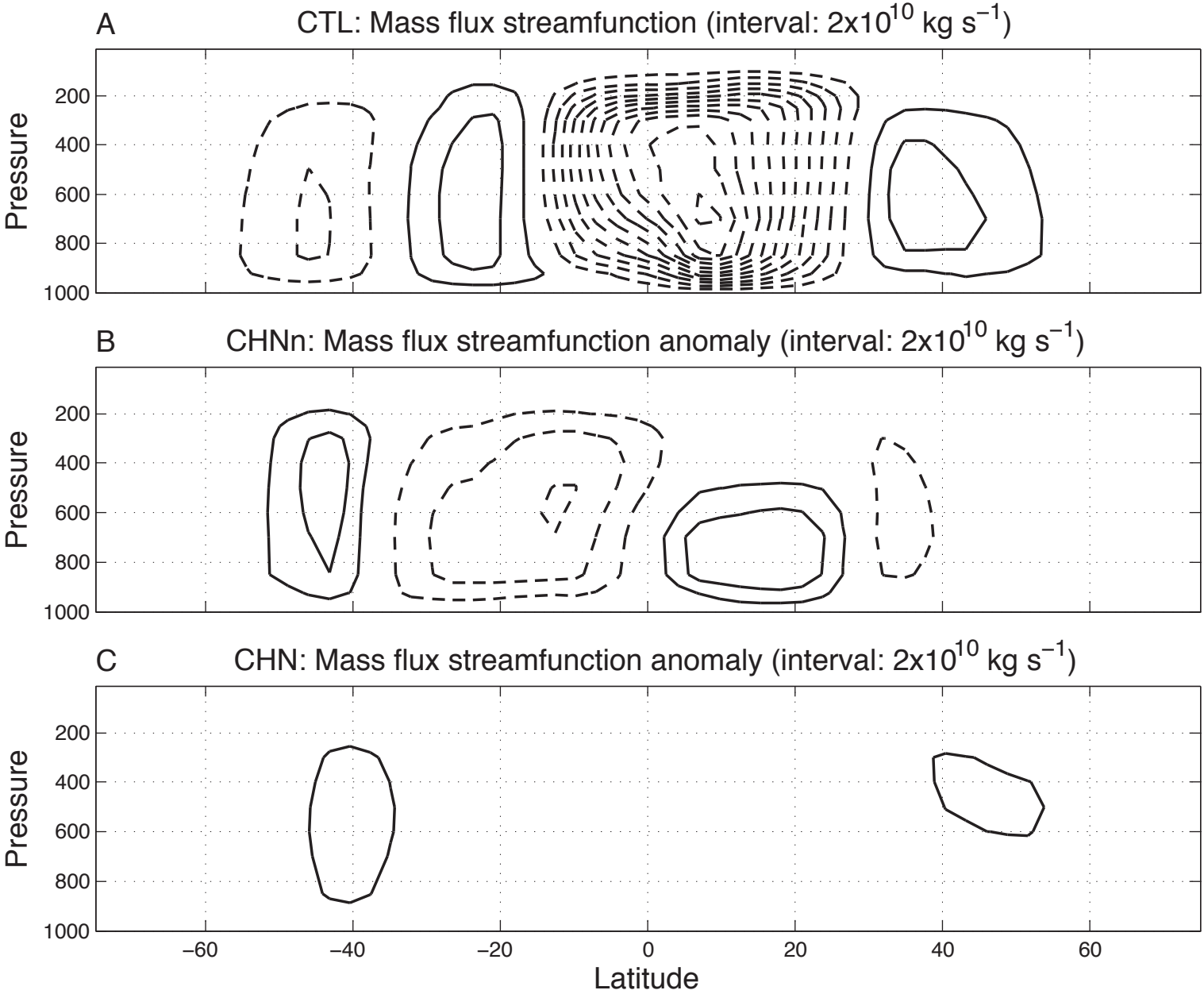
A
CTL: Mass flux streamfunction (interval: 2x10^10 kg s^−1)
B
CHNn: Mass flux streamfunction anomaly (interval: 2x10^10 kg s^−1)
C
CHN: Mass flux streamfunction anomaly (interval: 2x10^10 kg s^−1)
Pressure
200
400
600
800
1000
−60
−40
−20
0
20
40
60
Latitude